Paper No. 2031. (quote when citing this article)
Eleventh World Conference on Earthquake Engineering
ISBN: 0 08 042822 3

SITE EFFECTS OBSERVED DURING THE HYOGO-KEN NANBU EARTHQUAKE OF 1995 AND STRONG MOTION SIMULATION INCLUDING THE BASIN-EDGE EFFECT

H. KAWASE

Izumi Research Institute, Shimizu Corp., Fukoku Seimei Bldg, 2-2-2, Uchisaiwai-cho, Chiyoda-ku, Tokyo, 100 Japan

ABSTRACT

The devastating damage in Kobe and surrounding areas from the Hyogo-ken Nanbu earthquake of 1995 is caused by unfortunate coordination of the source effect with the strong site effects. On the source side rupture process inversions reveal that rupture propagation toward Kobe, the so-called forward directivity, is responsible to generate very strong 1 Hz pulses in the fault-normal direction. These pulses are then amplified by a two-dimensional basin-edge structure extending in the direction of the Rokko faults. In addition to the direct S-wave that is amplified by 100% (x 2.0), the basin-induced diffracted/surface waves contribute another 50% of amplification (x 1.5) in the area 0.5 km to 1 km away from the edge, and therefore our estimated peak ground velocity in this narrow zone reaches to 150 cm/sec at maximum. The soft surface layers, which are forced to behave nonlinearly, may give additional 30% of amplification in the area but may deamplify ground motions in the area close to shorelines and in the reclaimed land due to liquefaction to prevent severe damage there. We call the constructive interference near a sharp edge of a basin as "the basin-edge effect."

KEYWORDS

site effects; soil nonlinearity; simulation; effective stress analysis; basin-edge effect; surface waves; strong motion; bedrock motion; Kobe; the 1995 Hyogo-ken Nanbu earthquake

INTRODUCTION

The Hyogo-ken Nanbu earthquake of 1995 caused devastating damage to Kobe and surrounding areas. To understand the cause of the damage first we need to quantify the strength of input motions to structures in the area during the earthquake. After the earthquake different institutions launched damage survey teams to Kobe and unanimously found that heavily damaged buildings and collapsed residential houses were concentrated in a narrow zone to form so-called "the damage belt" in the direction from WSW to ENE. This strike coincides with that of the Rokko geological faults and the seismogenic fault plane until Nada-ward (AIJ, 1995). Further to the east the damage belt starts to bend southward and departs from the fault strike, but it still goes along the southern end of the Rokko geological faults. Thus it is quite natural to attribute the formation of the damage belt to the strong site effects there, however, the reality does not seem to be so simple as our first thought.

At first a lot of geologists and tectonophysicists had attributed the damage concentration to the strong fault rupture near the surface in the Kobe side, as was the case in the Awaji side. After detailed investigation it turns out that no surface breaks along the Rokko geological faults seem to exist (Awata *et al.*, 1995). Also the damage belt lies 500m-1,000m away from these faults, which cannot be explained by the rupture near the surface on these faults. Several researchers hypothesized that the rupture of an unknown buried fault just below the damage belt might cause such concentration. However, fault process inversions (e.g., Wald, 1995; Sekiguchi *et al.*, 1995) unanimously show that slip on the Kobe-side segment is concentrated in a deeper part

(≤10km) so that such a buried fault, even if exist, could not generate high acceleration in the limited area on the surface. Aftershock distribution also contradicts to this buried fault hypothesis.

On the other hand several earthquake engineers insist that shallow surface soils be responsible to the damage concentration in Kobe. In fact aftershock observation reveals that strong amplification more than 10 times at stations inside the damage belt relative to a rock site exists (AIJ, 1995). Shallow surface layers should amplify input motions but the problem is that we cannot find any characteristic structures that may cause the observed damage concentration. Others attribute it to the irregularity in a shallow soil structure (Adam and Takemiya, 1995). However, the ground shaking was too strong to have such a strong effect of irregularity in soft layers because its nonlinear behavior prevents lateral interaction and subsequent horizontal wave propagation, as demonstrated by a nonlinear analysis in Higashinada ward, Kobe (Kawase *et al.*, 1995). We have already proposed an alternative answer that not only explains the damage belt but also reproduces observed strong motions quantitatively. Here we would like to summarize essential facts that we have learned from studies on the effects of surface geology in Kobe during the Hyogo-ken Nanbu earthquake.

OBSERVED DATA AND SOURCE CHARACTERISTCS

To understand the source characteristics of the main shock Irikura and Fukushima (1995) plot the observed peak ground acceleration (PGA) and velocity (PGV) as a function of minimum fault distance, together with the empirical attenuation curves. Fig.1 shows their plot to find nothing anomalous in either PGA or PGV. In another word it is difficult to attribute the severe damage in Kobe to its average source characteristics.

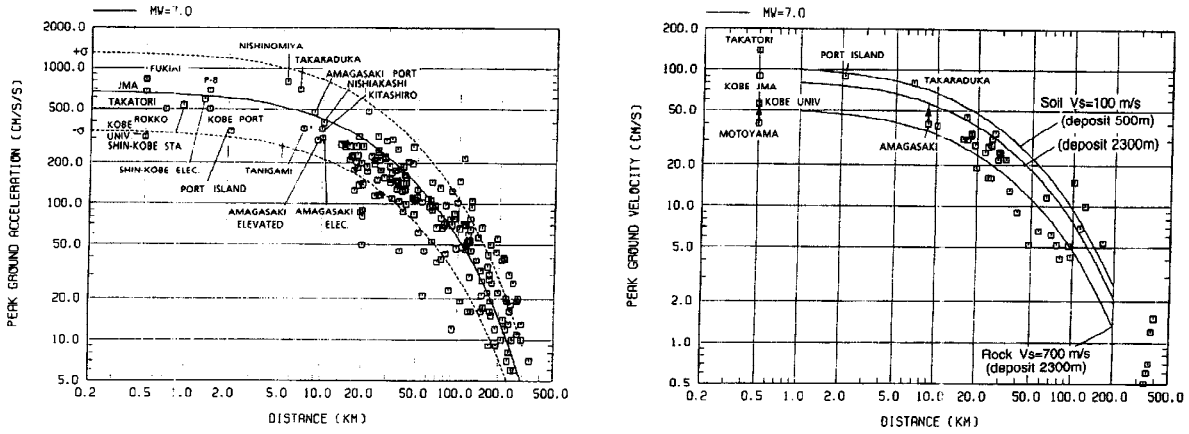

(a)Peak Ground Acceleration (b)Peak Ground Velocity

Fig.1 (a) PGA and (b) PGV distributions of observed horizontal records during the 1995 Hyogo-ken Nanbu earthquake and empirical attenuation curves (Irikura and Fukushima 1995).

As stated above source inversion studies unanimously found that three major areas with large slip (asperities) exist on the fault plane, one at the shallow part in the Awaji side, another near the hypocenter, and the other 10km below central Kobe. Although such studies restrict themselves to reproduce seismograms only in the frequency range lower than 1 Hz, they found that distinctive velocity pulses observed in Kobe are generated by the forward directivity of the fault rupture, as have been seen in the 1989 Loma Prieta earthquake and the 1994 Northridge earthquake (Somerville, 1996). Pseudo velocity response spectra of observed records at 4 stations (Fig.3) are plotted in Fig.2 for fault-normal and fault-parallel horizontal components. It is clear that the fault-normal components share the common predominant frequency of 1 Hz with very high peak values but that the fault-parallel components have considerably less amplitude than the fault-normal component. This is a direct consequence of nearfield directivity in the fault-normal component (Somerville, 1996). The central issue then is how to explain the strong site-dependency of peak values at around 1 Hz shown in Fig.2.

INVERTED BEDROCK MOTION AT JMA KOBE STATION

Fig.3 shows the damage belt in Kobe defined as the area of the JMA (the Japan Meteorological Agency) intensity scale VII, which means more than 30% of wooden houses were collapsed, together with major Rokko faults in the area. Several organizations succeeded to observe strong motions during the main shock at about 10 stations in total in Kobe, but unfortunately most of them are not inside the damage belt. Records collected by JMA were released to the public quite soon after the earthquake and so the record at the JMA Kobe meteorological observatory is most frequently used one for structural analyses. However, it is located only 80m southeast from the Egeyama fault, as shown in Fig.3, and is on a small hill of the weathered Osaka

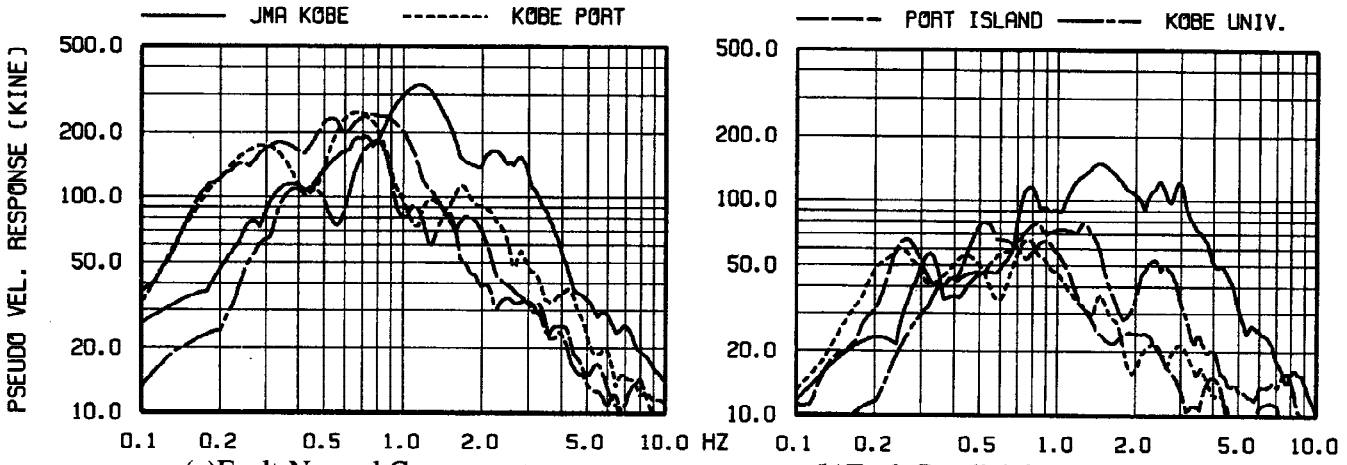

(a)Fault-Normal Component (b)Fault-Parallel Component

Fig.2 Pseudo velocity response spectra (5% damping) of (a) fault-normal and (b) fault-parallel components of the observed horizontal records at 4 stations around Sannomiya during the Hyogo-ken Nanbu earthquake.

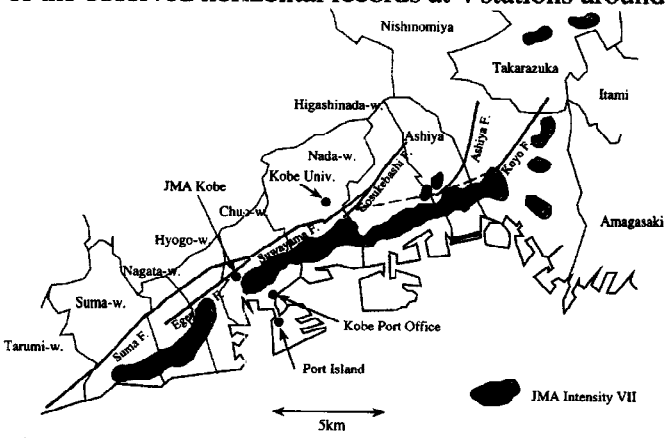

Fig.3 Damage belt distribution defined as the region of the JMA intensity scale VII, together with the Rokko geological faults. Solid circles denote major strong motion stations in the district.

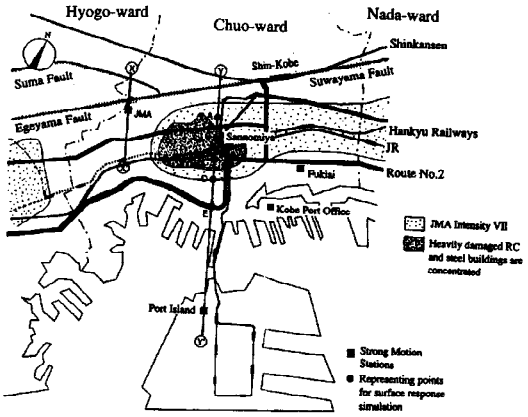

Fig.4 A map of Chuo-ward, downtown Kobe. It shows two model sections, x-x' section for the JMA deconvolution and y-y' section for the Sannomiya simulation. A to E are 1-D shallow soil analysis sites.

Group formation, which consists of mostly sand-and-gravel layers in the early Pleistocene, the record should be contaminated by complicated site effects. We evaluate the bedrock motion supposedly observed on the outcrop of the nearby Rokko granite using an appropriate ground structure represented by a two-dimensional finite element method (2-D FEM). We compare this bedrock motion with the observed record at Kobe University, which is on the Rokko granite side.

Fig.4 shows a simplified map of Chuo-ward, Kobe, around Sannomiya. It shows Suma, Egeyama, and Suwayama faults as well as two sections of model planes used for FEM analyses. The strike, N30°W, of these two sections is chosen based on a principal direction analysis of the JMA record and is close to the fault-normal direction. Since the basin-edge structure spreads two-dimensionally along the direction of the fault strike, that is, WSW-ENE direction, it is quite appropriate to represent it by a 2-D model subject to a plane body wave. The fault-normal component corresponds to an SH-wave as a radiated wave from the source, but to an SV-wave as an input to the geological structure.

Fig.5 shows an FEM model used for the JMA section. In this model we model two vertical geological faults at which vertical offsets to the bedrock are assumed to be 200m and 800m, respectively. Thicknesses and P- and S-wave velocities of three layers of the Osaka Group formation and a Pliocene layer below are assumed as such based on the geophysical exploration studies and borehole surveys conducted mainly in the Osaka plain. Those for Holocene and middle or late Pleistocene layers are estimated from the standard penetration test N-values of boring data. The horizontal extent of the FEM region is 800 m and transmitting and viscous boundaries are attached at both sides and at the bottom, respectively, to account for outgoing waves. The surrounding bedrock is assumed to have P- and S-wave velocities of 5,000 m/sec and 2,500 m/sec.

Once a frequency-domain response at the JMA station is calculated, an outcrop bedrock motion can be obtained as a deconvolution from the observed record. Fig. 6 shows the observed velocity record in the major axis (N32°W), the deconvolved bedrock motion in the same direction, and the velocity record in the major axis

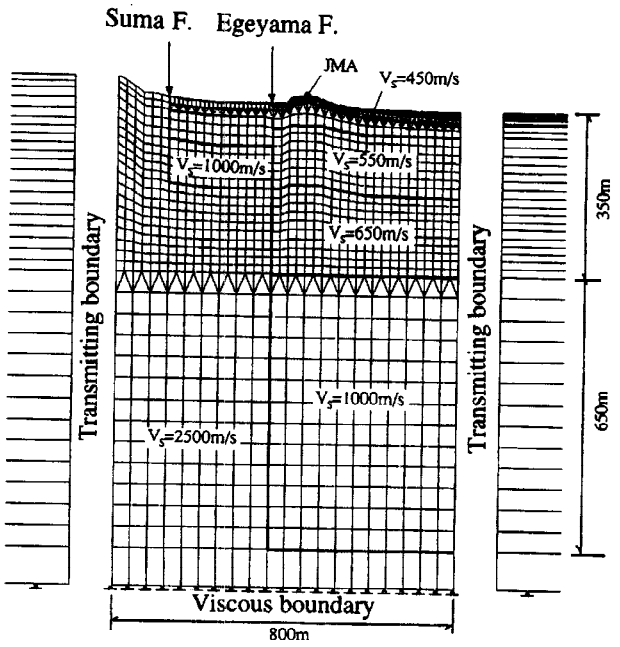

Fig.5 A two-dimensional FEM model for the deconvolution analysis at the JMA section. Shallow Holocene and middle or late Pleistocene layers on the deep basin structure are considered.

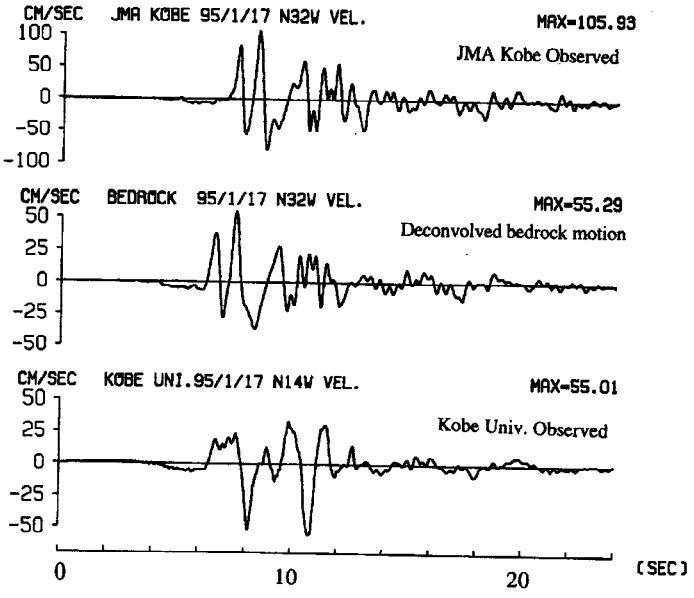

Fig.6 Comparison of the observed velocity record at JMA Kobe (N32°W), the calculated bedrock motion, and the observed record at Kobe University (N14°W). The amplitudes are quite similar in the latter two.

(N14°W) observed at Kobe University (Toki *et al.*, 1995), which is shown for comparison. By removing the effects of the basin and surface soils PGV decreases to about one half and becomes very close to that at Kobe University (PGA, 335 cm/sec^2, is close, too). Their spectra are also similar to each other. Thus this bedrock motion seems to be reasonable within an error of 20 to 30% associated with the model uncertainty.

STRONG MOTION SIMULATION IN SANNOMIYA, DOWNTOWN KOBE

Next using the calculated bedrock motion we simulate ground motions on the outcrop of the Osaka Group formation by using a simple 2-D FEM again which represents a geological structure beneath the Sannomiya section. Ground motions on the actual surface can be evaluated later by 1-D nonlinear analyses of surface layers. Fig.7 shows an FEM model used to calculate responses on the outcrop of the Osaka Group formation. We only model three layers of the Osaka Group formation and one Pliocene layer below, whose material properties are the same as those of the JMA section. The total model width is 3,960m. At the Suwayama fault, which is 160m away from the left FEM boundary, we give a vertical offset of about 1,000m.

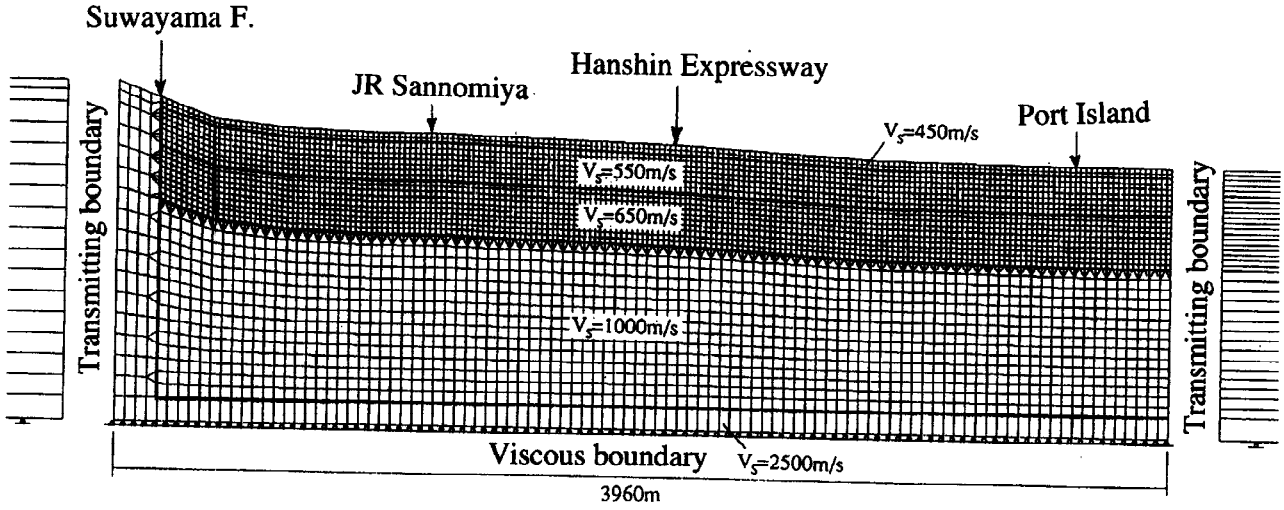

Fig.7 A two-dimensional FEM model for the simulation analysis along the Sannomiya section y-y' shown in Fig.4. No soft surface layers are modeled at this time.

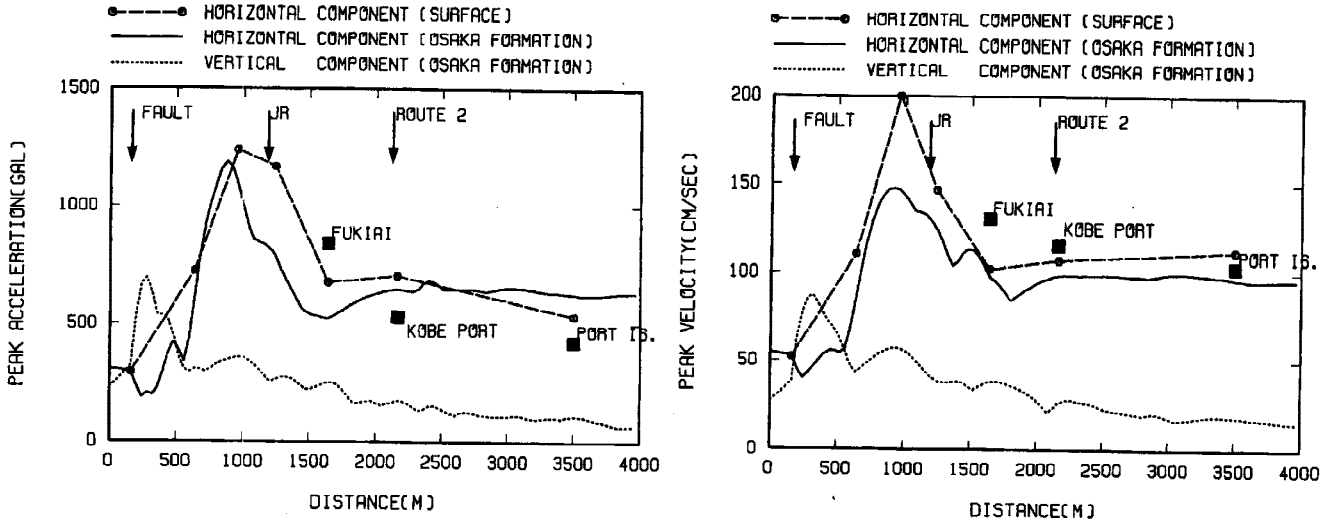

Fig.8 Distributions of (a) PGA and (b) PGV along the surface of the 2-D FEM model for Sannomiya section. The bedrock motion shown in Fig.5 is used as an input. Solid curves denote the horizontal (fault-normal) responses while dotted curves denote the vertical ones. Broken lines with circles show peak values along the surface of the Holocene layers that cover the 2-D FEM surface. Solid squares denote the observed values.

Acceleration and velocity responses along the surface of the Sannomiya section are calculated and their peak values are plotted in Fig.8. Horizontal components have a prominent peak at about 900m (740m from the fault) where its PGA and PGV reach to 1,200 cm/sec^2 and 150 cm/sec, respectively. Around the peak we have a 600m wide region in which PGAs and PGVs are exceeding 800 cm/sec^2 and 120 cm/sec. From about 2,000m to the south the peak level converges to a uniform value that corresponds to the 1-D response of the basin structure. This means that the 1-D response draws a bottom line to have 100% amplification (=twice) with respect to the input. The 2-D basin effect is prominent only in the region within 1,200m from the edge to give us additional amplification of 50% (=1.5 times; 3 times in total). Interestingly, in the region very close to the fault vertical components have peak values higher than the horizontal ones. Since no vertical input is applied here, vertical responses are purely associated with the 2-D basin effect.

Although peak value distributions at this stage are for the imaginary surface of the Osaka Group formation, it is clear that the 2-D effect is strong enough to have additional amplification of 50% on top of the 1-D response. The region of high peak acceleration and velocity roughly corresponds to the observed damage belt shown in Figs.3 and 4, though its width seems a little narrower than the observed. To fill the gap we need to consider shallow soil responses that will be shown next.

SIMULATION OF SHALLOW SOIL RESPONSES

Since simulated motions on the surface of the Osaka Group formation are so intense, we should use a nonlinear liquefaction analysis that takes into account the effects of excess pore water pressure (Kawase *et al*, 1996). If we consider such nonlinear responses of shallow Holocene and middle or late Pleistocene layers we have another amplification of 30 to 50% to have a wider size of the high-amplitude region. We have obtained quite good agreement between the calculated seismograms and the observed ones at Fukiai Gas Station, Kobe Port Office, and Port Island. Here we show a comparison at Port Island as an example. Then we show surface responses at five representing points, A to E, along the Sannomiya section in Fig.4.

Port Island is a big reclaimed land, about 2 km by 2 km wide, as shown in Figs.3 and 4. The strong motion observation site at the northwestern corner of the island has three borehole stations and one surface station. As have already reported by a lot of news articles and research papers, Port Island suffered heavy damage from liquefaction and subsequent land slide and settlement. Detail parameters and description of the analyzing method used here can be found in Kawase *et al.* (1996). Since the observed strong motions at the Port Island station are also strongly polarized to the fault-normal direction, N32°W~N35°W, we can use simulated outcrop motion as an input at the deepest station 83m below the surface. Fig.9 shows a comparison of the observed and simulated seismograms at all the four stations, namely, the surface (GL), GL-16m, GL-32m, and GL-83m. The agreement is remarkably good considering the lengthy simulation process adopted here.

Based on the successful reproduction of the observations at Port Island as well as other stations in the region such as Fukiai Gas Station or Kobe Port Office, we proceed to simulate strong motions in the damage belt

where no observed records are available. Parameters of shallow Holocene and middle or late Pleistocene layers at each point are assumed referring to boring data at nearby sites. The resultant PGAs and PGVs of horizontal component are plotted in Fig.8 by broken lines with solid circles on top of the peak values on the outcrop of the Osaka Group formation. The observed peak values on the surface are also plotted by solid squares. As a result of shallow soil amplification we have now about 1 km wide high PGA (≥800 cm/sec^2) and PGV (≥120 cm/sec) region. Peak value begins to emerge high at about 500 m from the fault, peaks out at 840 m, and converges to the 1-D values at about 1,500 m. PGA at the peak do not change much, about 1,200 cm/sec^2, while PGV is increased about 30% to become 200 cm/sec. Note that PGA is decreased at Port Island (GL) because of complete liquefaction in the artificially filled sand-and-gravel layers.

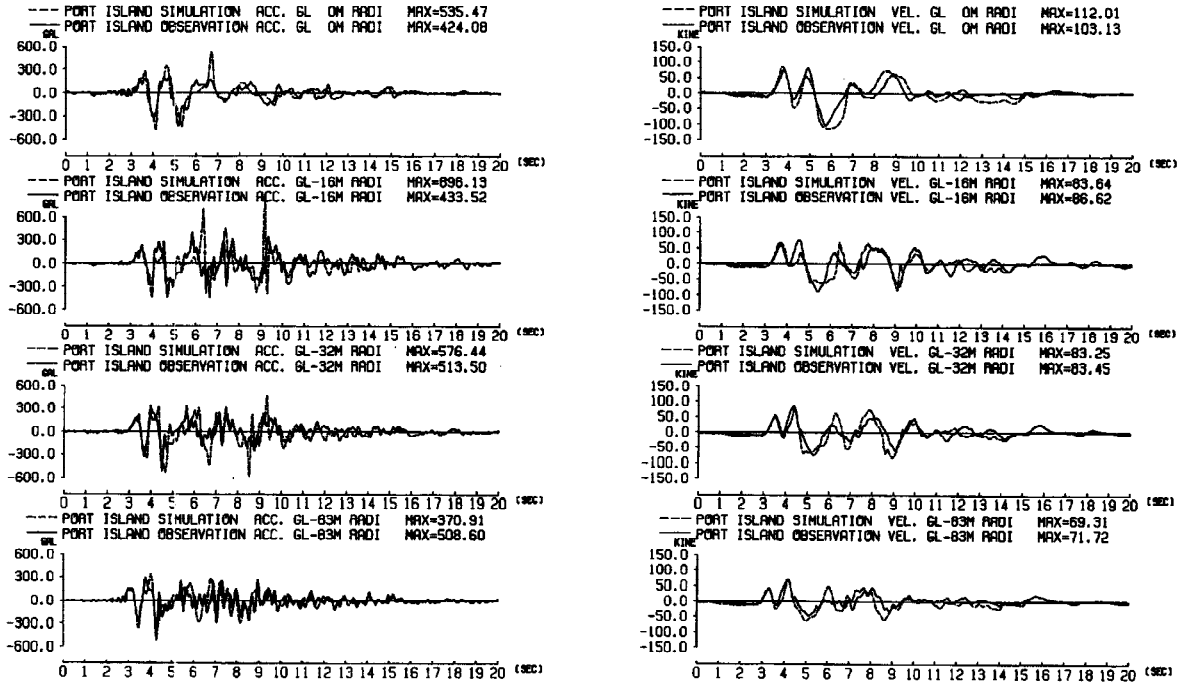

Fig.9 Acceleration and velocity seismograms at the Port Island stations at GL, GL-16m, GL-32m, and GL-83m, observed (solid curves) and simulated (dotted curves).

THE BASIN-EDGE EFFECT

We have shown that the 2-D effect near the basin edge should be a primary cause of the damage belt in Kobe. The only important question yet to be answered is how such high amplification emerges in such a narrow region close to the edge. Since a basin model shown in Fig.7 has a curved surface that gives us additional complexity in the wave propagation, we use a simpler model with flat layers whose thicknesses and P- and S-wave velocities are taken from that model. The bedrock motion is also too complex so that we use as an input a Ricker wavelet with the characteristic frequency of 1 Hz, the predominant frequency of the bedrock motion.

Fig.10 shows snapshots of the response of this rectangular basin. To have a closer look on the wave propagation near the edge we take a region of 2.4 km wide and 1.2 km deep. One tick mark in both axes corresponds to 400 m. The boundary between the surrounding bedrock and the sediments is shown by dashed lines. Contours are made for both horizontal and vertical responses of the basin to a Ricker wavelet with normalized peak amplitude. Note that a Ricker wavelet takes a peak in the minus side that is expressed by solid black.

At t=2.0 the peak of a Ricker wavelet is assigned to hit the bottom of the basin. It takes less than 0.5 second for the direct S-wave to pass through the surrounding rock, while it does about 1.4 seconds inside the basin. Therefore at about t=2.5 the peak in the rock reaches to the surface, long before the peak in the basin shows up, and it emits a strong phase of diffracted wave into the basin due to a displacement discontinuity at the edge. After the diffracted wave started to propagate in the horizontal direction, the peak in the basin keeps approaching toward the surface. When the peak in the basin hits the surface at t=3.5, the peak of the horizontally propagating wave is located at 1km away from the edge where the maximum amplification is obtained. After this constructive interference occurred, the direct S-wave reflects back to the bottom and the horizontally propagating wave keeps going to the right with changing its sign as shown in the snapshots at t=4.0 and t=4.5. We can see more clearly the sign change in the vertical component. The sign change is a

very characteristic nature of dispersive surface waves. The same sign of wave is propagating by the phase velocity, while the energy centroid is propagating by the group velocity, irrespective of the sign. Theoretical dispersion analysis of the 1-D basin structure shows that in the horizontal component the first higher mode of Rayleigh wave with the phase velocity of about 1km/sec will be dominant, while in the vertical component the fundamental mode with the phase velocity of about 500m/sec will be, which coincide with the apparent velocities of these waves seen in the snapshots. We should also note that the amplitudes of these waves are concentrated only in a relatively shallow part of the basin. These relevant pieces of information systematically suggest that the main portion of the horizontally propagating waves consist of Rayleigh wave soon after the departure from the edge. Thus we can conclude that the amplification at around 1km away from the basin edge is caused by the coincidental collision of the direct S-wave with the basin-induced diffracted/surface waves that is generated at the edge and radiated horizontally. We call this special amplification effect as "the basin-edge effect" to emphasize that it should concern engineers who design structures near a sharp edge of a basin.

Natural but important consequence of this interpretation is that a) if the basin were deeper, then the location of the damage belt would be further away from the edge because the direct S-wave needs more time to appear on the surface and hence the surface wave goes further till rendezvous, and b) if the predominant frequency of the input were higher, then the location of the damage belt would be much closer to the edge because the velocity of the surface wave becomes slower and hence they does not go further till rendezvous. In either case the impact of the edge effect will be smaller since traveling in a long distance or by a high-frequency wave make attenuation larger. If the mechanism of the basin-edge effect is not the one elucidated here but something like a focusing effect of body waves suggested by others (Shichi and Aoki, 1995; Motosaka and Nagano, 1995), then the location of amplification should be geometrically determined and so frequency independent. For input motions with different characteristic frequencies we observe the phenomena exactly as described above.

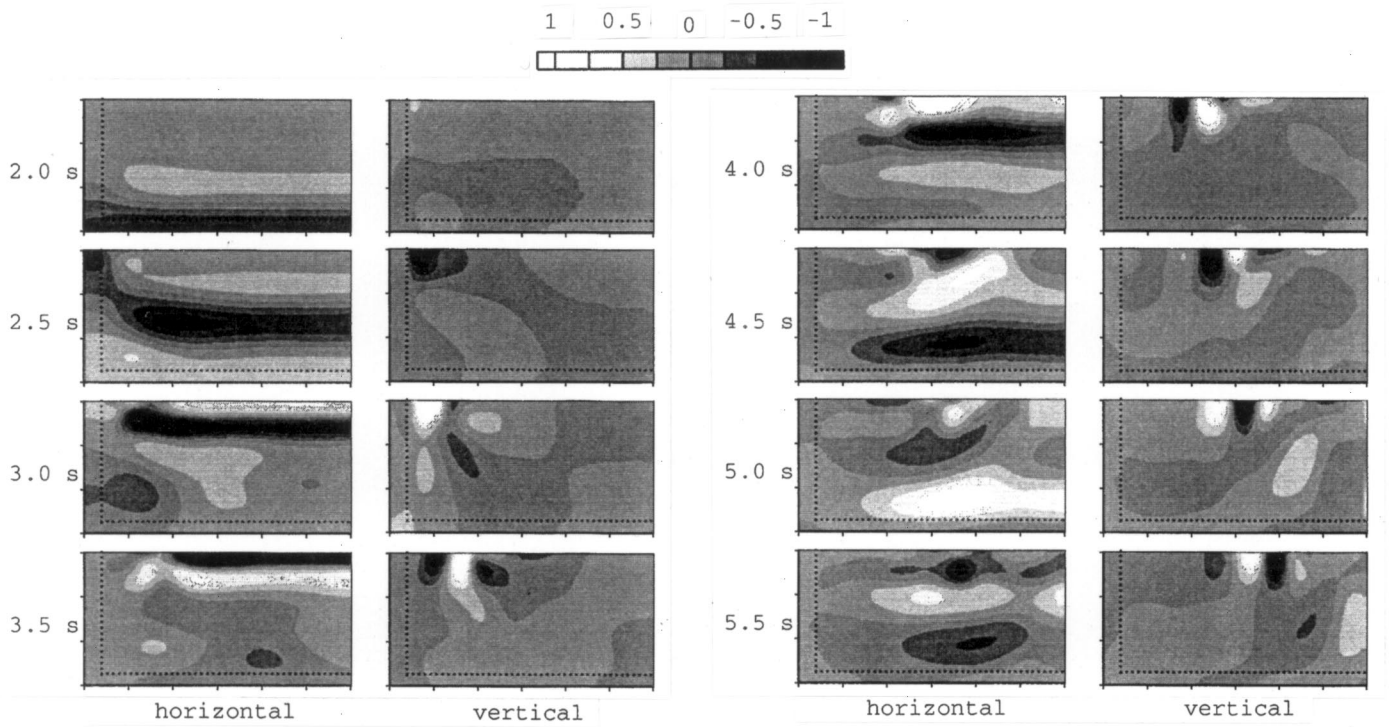

Fig.10 Snapshots of the 2-D rectangular basin response for every 0.5 second as contour maps. Input is a 1 Hz Ricker wavelet normalized to have an amplitude -1.0 at its peak.

CONCLUSIONS

We summarize the most important aspects of the strong motion characteristics observed during the Hyogo-ken Nanbu earthquake of 1995. First we discussed its source characteristics and subsequent nearfield bedrock motion characteristics. Then we try to reproduce strong ground motions in the Sannomiya district, downtown Kobe, in order to understand the real cause of the damage belt extending along the strike of the Rokko geological faults. We use the resultant bedrock motion as an input to a simple 2-D FEM model for the Sannomiya section with only early Pleistocene and Pliocene layers. A region of high amplification appears in the same location with the observed damage belt during the main shock. We then show results of 1-D nonlinear shallow soil analyses and compare them with the observed records to validate our simulation process. Finally to elucidate the mechanism of the high amplification near the basin-edge we show snapshots of the basin response to a 1 Hz Ricker wavelet input. From these results we conclude the following:

(1) The observed PGA and PGV do not show any anomalous features on the average. However, the near-field strong motion records show distinctive characteristics, namely strong velocity pulses with the predominant frequency of 1 Hz. Source process studies reveal that the forward directivity contributes to amplify them.
(2) The estimated bedrock motion from the JMA station record has PGA and PGV of 335 cm/sec^2 and 55 cm/sec, respectively, which are similar to those observed at Kobe University and are not particularly high.
(3) Simulated outcrop motions on the early Pleistocene layers along the Sannomiya section show the largest peak values, 1,200 cm/sec^2 in PGA and 150 cm/sec in PGV, at 740 m away from the basin edge. Around this maximum point they have peak values more than 800 cm/sec^2 and 120 cm/sec, respectively. The location and the width of this high amplitude region roughly correspond to those of the damage belt during the main shock.
(4) Using shallow soil responses calculated by a 1-D nonlinear liquefaction analysis we can successfully simulate observed strong motions. We estimate the maximum ground motions inside the damage belt to be 1,200 cm/sec^2 in PGA and 200 cm/sec in PGV. Strong liquefaction in the area close to shorelines and in the reclaimed land may deamplify ground motions and prevent severe damage there.
(5) The simulated high amplitude region is caused by the coincidental collision of the direct S-wave with the basin-induced diffracted/surface waves generated at the basin edge. We call this type of site effects near a sharp edge of a basin subject to an incident body wave as "the basin-edge effect."

ACKNOWLEDGMENTS

Strong motion records at the JMA Kobe station, Kobe University, Fukiai Gas Station, Kobe Port Office, and Port Island were observed by JMA, the Committee for Earthquake Observation and Research in Kansai Area, Osaka Gas Co., Port and Harbor Research Inst., and City of Kobe, respectively. Efforts of the persons-in-charge for their observation and prompt delivery are highly appreciated. The author is grateful to the discussion with Prof. Irikura, Dr. Iwata, Ms. Sekiguchi, Mr. Pitarka, Prof. Kamae, and Dr. Somerville. Special thanks are given to Drs. Hayashi, Satoh, Matsushima, and Fukutake for their help in the analyses.

REFERENCES

Adam, M. and H. Takemiya (1995). Why heavy seismic damage has concentrated at a specific area for the Sanyo Shinkansen line viaduct ?, Proc. of the 50th Annual Meeting of the Japan Society of Civil Eng., Vol.I, 1232-1233.

Architectural Institute of Japan (1995). Preliminary reconnaissance report of the 1995 Hyogoken-Nanbu earthquake, English edition, Architectural Institute of Japan, Japan.

Awata, Y., K. Mizuno, Y. Sugiyama, R. Imura, K. Shimokawa, K. Okumura, K. Kimura, and E. Tsukuda (1995). Surface fault ruptures associated with the Hyogo-ken Nanbu (Kobe) earthquake of 1995, Japan, EOS, Transaction of AGU, **76**, No.46, S21F-8.

Irikura K. and Y. Fukusima (1995). Attenuation characteristics of peak amplitude in the Hyogoken-nambu earthquake, J. Nat. Disaster Sci., **16**, No.3, 39-46.

Kawase, H., T. Satoh, S. Matsushima, and K. Irikura (1995). Ground motion estimation in the Higashinada ward in Kobe during the Hyogo-ken Nambu earthquake of 1995 based on aftershock records, J. Struct. Constr. Eng., AIJ, **476**, 103-112 (in Japanese).

Kawase, H., T. Satoh, and K. Fukutake (1996). Simulation of the borehole records observed at the Port Island in Kobe, Japan, during the Hyogo-ken Nanbu earthquake of 1995, 11th WCEE, Acapulco, Mexico.

Motosaka, M., and M. Nagano (1995). Effects of deep irregular underground structure and shallow surface geology on the amplification characteristics of ground motions in Kobe City during the 1995 Hyogo-ken Nanbu earthquake, -Analytical study on interpretation of the heavily damaged belt zone-, EOS, Transaction of AGU, **76**, No.46, S21F-12.

Sekiguchi, H., K. Irikura, T. Iwata, Y. Kakehi, and M. Hoshiba (1995). Minute locating of fault planes and source process of the 1995 Hyogo-ken Nanbu (Kobe), Japan, earthquake from the waveform inversion of strong ground motion, EOS, Transaction of AGU, **76**, No.46, S22B-13, also submitted to J. Phys. Earth.

Shichi, R. and H. Aoki, 1995, Gravity anomaly in the rupture zone of the 1995 Hyogo-ken Nambu earthquake (translated from the Japanese title), Chikyu Monthly, Special issue for the 1995 Hyogo-ken Nambu earthquake, Kaiyo Shuppan, No.13, 129-134 (in Japanese).

Somerville, P.G. (1996). Forward rupture directivety in the Kobe and Northridge earthquakes, and implication for structural engineering, Proc. 7th US-Japan Workshop on the Improvement of Struct. Design and Constr. Practices, JSCA and ATC, Jan. 18-19, 1996, Kobe, Japan.

Toki, K., K. Irikura, and T. Kagawa (1995). Strong motion records in the source area of the Hyogoken-nambu earthquake, January 17, 1995, Japan, J. Nat. Disaster Sci., **16**, No.2, 23-30.

Wald, D.J. (1995). A preliminary dislocation model for the 1995 Kobe (Hyogo-ken Nanbu), Japan, earthquake determined from strong motion and teleseismic waveforms, Seism. Res. Lett., **66**, No.4, 22-28.